Three-Dimensional Monte Carlo Simulation of Grain Growth in the Heat-Affected Zone of a 2.25Cr-1Mo Steel Weld

S. SISTA, Z. YANG, and T. DEBROY

We report here the first three-dimensional (3-D) Monte Carlo (MC) modeling of grain growth in the heat-affected zone (HAZ) of a weldment. Computed grain-size distributions in the HAZ of a 2.25Cr-1Mo steel, for different heat inputs in the range from 1.1 to 4.8 MJ/m, were compared to independent experimental results. The simulated mean grain size for different heat inputs agreed well with the corresponding independent experimental data. The mean grain size at various locations equidistant from the fusion line were different. The predicted grain size from the 3-D model matched the experimental results more closely than that from a two-dimensional (2-D) model. When the whole calculation domain was subjected to a single thermal cycle experienced by a monitoring location within the HAZ, the computed grain size was larger than that calculated at the monitoring location by taking into account the prevailing temperature gradient due to thermal pinning. The good agreement between the simulated grain structure and the corresponding experimental results indicates significant promise for understanding grain-growth phenomena in the entire HAZ by using the MC technique.

I. INTRODUCTION

THE driving forces for grain-size change are classified into two categories. The reduction of grain-boundary energy (or curvature) leads to normal and abnormal grain growth. The reduction of internal defects also leads to changes in grain size due to static and dynamic recrystallization. In most alloys, grain growth occurs due to a reduction in grain-boundary curvature.[1,2,3] Computer simulation has been used in recent years to quantitatively study grain growth. In particular, the Monte Carlo (MC) simulation has been widely used to simulate the grain structure under isothermal conditions.[4–7] Apart from grain-growth kinetics, MC simulations also provide information on the evolution of grain morphology which cannot be obtained by analytical equations.[4–7] Recently, MC calculations have also been used to simulate the grain growth in the heat-affected zone (HAZ) of welds.[8–11]

In MC simulations, the dimensionless grain size changes with the number of iterations, which is also known as the MC simulation time steps (t_{MCS}). In the MC model, the grain-size variation with t_{MCS} is largely independent of material properties and real-time grain-growth kinetics and is only dependent on the grid system (*e.g.*, the dimensions of the system and total number of grid points). In order to quantitatively predict grain growth for a specific material under given thermal conditions, a relation needs to be established between the simulation steps, t_{MCS}, and real time. So, a kinetic submodel is needed to simulate grain growth using the MC technique.

Previous work on modeling grain growth in the weld HAZ using MC simulation included two approaches in relating the t_{MCS} to the real time. Radhakrishnan and Zacharia[10] and Wilson *et al.*[11] modeled grain growth in the weld HAZ by considering a linear relationship between t_{MCS} and real time. Gao *et al.*[9] suggested that there was insufficient evidence to show that the MC simulation time could be linearly related to the real time in all material systems. They proposed three models—the atomistic model, the experimental data–based (EDB) model, and the grain-boundary migration (GBM) model—to relate t_{MCS} and real time to address various situations.

One common feature in all the previous work done by both the groups was that the simulation was two-dimensional (2-D) in what was really a three-dimensional (3-D) HAZ. Considering the significant local-temperature gradients in all directions in the HAZ, 2-D simulation of grain growth is inadequate. Furthermore, the width of the HAZ usually varies with the location in the actual weldment. This variation cannot be accounted for in the 2-D simulations, and 3-D calculations are needed for a realistic simulation. The phenomenon of "thermal pinning," in which a grain is physically restricted from growing due to steep temperature gradients in all the three directions, is more effectively modeled in 3-D than in 2-D simulations. Thus, a 3-D MC model needs to be developed which incorporates both the presence of steep temperature gradients and spatially dependent thermal cycles and also the nonlinear nature of the relation between t_{MCS} and real time.

There are considerable computational challenges in conducting meaningful MC calculations. The main challenge is in the processing of a large volume of data in a realistic time frame. For example, a 2-D grid of 40 × 1550 grid points with 80 iteration steps involves about 5 million (40 × 1550 × 80) data points. Only in recent years have such large-scale computations become tractable, because of advances in computational hardware. On the other hand, with a more-realistic 3-D calculation with 40 × 1550 × 1550 grid points undergoing 80 iteration steps, the number of data points increases to about 7.7 billion. This three-orders-of-magnitude increase in the volume of data presents several interesting challenges even for the most powerful modern computers. In particular, modern data visualization techniques and tools have to be pushed to their limits just

S. SISTA, Z. YANG, Graduate Students, and T. DEBROY, Professor, are with the Department of Materials Science and Engineering, The Pennsylvania State University, University Park, PA 16802.

Manuscript submitted October 29, 1999.

to visualize the computed results, even in an efficient binary format.

Here, we report the first comprehensive effort to develop a model to simulate grain growth in three dimensions in the entire HAZ of a fusion weld. As an example, grain growth in the HAZ of a 2.25Cr-1Mo steel weldment is simulated for various heat inputs. The model predictions are then compared to independent experimental results.[12] This steel is widely used in turbine engines, power generation equipment, and high-temperature applications because of its good corrosion and creep resistance.[3,11–14] Alberry and Jones[3,12,13] studied in detail the susceptibility to reheat cracking in these alloys and found that the increase in austenite grain size during service at high temperatures contributes to a significant reduction in the strength of the HAZ of these steels.

II. SIMULATION MODEL

A. *The MC Simulation of Grain Growth*

The application of the MC technique to model grain growth has been described in the literature.[4–10,19,20] Only the salient features pertinent to the specific problem addressed in this article are described here. Each grid point is assigned a random orientation number between 1 and Q, where Q is the total number of grain orientations. A grain-boundary segment is defined to lie between two sites of unlike orientation. In other words, two adjacent grid points having the same orientation number are considered to be a part of the same grain; otherwise, they belong to different grains. The grain-boundary energy is specified by defining an interaction between nearest-neighbor lattice sites. The local interaction energy (E) is calculated by the Hamiltonian:

$$E = -J \sum_{j=1}^{n} (\delta_{S_i S_j} - 1) \qquad [1]$$

where J is a positive constant which sets the scale of the grain-boundary energy, δ is the Kronecker's delta function, S_i is the orientation at a randomly selected site i, S_j is the orientation of its nearest neighbors, and n is the total number of the nearest-neighbor sites. The sum is taken over all nearest neighbors. Each pair of nearest neighbors contributes J to the system energy when they are of unlike orientation, or zero otherwise.

The kinetics of grain-boundary migration are simulated by selecting a site randomly and changing its orientation to one of the nearest-neighbor orientations, based on an energy change due to the attempted orientation change. The probability of the orientation change is defined as

$$p = 1 \text{ for } \Delta E \leq 0 \qquad [2]$$

$$p = e^{\frac{-\Delta E}{k_B T}} = e^{\frac{-(n_1 - n_2)J}{k_B T}} \text{ for } \Delta E > 0 \qquad [3]$$

where ΔE is the energy change, k_B is the Boltzman constant, J is a positive constant that sets the scale of the grain-boundary energy, T is the temperature, and n_1 and n_2 are the number of neighbors with different orientations before and after the attempted reorientation. The term $J/k_B T$ is taken to be equal to unity in this article (refer to Appendix 1). Thus, successful transitions at the grain boundaries to orientations of nearest-neighbor grains corresponds to boundary migration.

Through the MC simulation, an empirical relation between the simulated grain size and the MC simulation time can be obtained as[8,9]

$$L = K_1 \times \lambda \times (t_{MCS})^{n_1} \qquad [4]$$

which can be written as

$$\log\left(\frac{L}{\lambda}\right) = \log(K_1) + n_1 \log(t_{MCS}) \qquad [5]$$

where L is the simulated grain size measured by mean grain intercepts, λ is the discrete grid-point spacing in the MC technique, t_{MCS} is the MC simulation time or MC simulation iteration steps, and K_1 and n_1 are the model constants, which are obtained by regression analysis of the data generated from MC simulation. It should be noted that Eq. [4] represents the intrinsic grain-growth kinetics of the MC model, dependent only on the grid system of the MC model and largely independent of the material properties and temperature-time history. The MC simulation time in Eq. [4] is a dimensionless quantity.

B. *Application of MC Technique in the HAZ of Real Welds*

To apply the MC-based grain-growth simulation technique to welding, the conversion of the MC simulation step (t_{MCS}) to real time–temperature is necessary. Radhakrishnan and Zacharia[10] related t_{MCS} to real time and temperature as

$$t_{mcs} = K_1 K_2^0 te^{\left(-\frac{Q_M}{RT}\right)} \qquad [6]$$

The symbol K_1 was a scaling constant between MC space and real space and is given by

$$K_1 = \frac{D_R}{D_M} \qquad [7]$$

where D_R is the real grain size and D_M is the dimensionless MC simulated grain size (measured in number of grid spacings). Thus, K_1 corresponded to the grid spacing, which could be assumed according to the situation. The symbol K_2^0 is an empirical "frequency factor," Q_M is the activation energy for grain-boundary migration, R is the gas constant, T is the temperature, and t is the real time. Both K_2^0 and Q_M were obtained from isothermal experimental measurements at different temperatures. The thermal cycles at various locations were incorporated into the model by breaking down a cycle at a given location into a number of small isothermal steps using a small time-step.

Gao *et al.*[8,9] questioned the linear relationship between the MC simulation time and real time and proposed three models (*e.g.*, the atomistic model, the GBM model, and the EDB model) to relate t_{MCS} and real time. The atomistic model can only be applied to small assemblies of atoms such as nanocrystals. Considering the large size of the HAZ, the atomistic model is not suitable for simulation of grain growth in this region. In the GBM and EDB models, the grid points are treated as a block of physical area, in a 2-D simulation, or of volume, in a 3-D simulation, in the material. When the isothermal grain-growth kinetics of a material are available, the EDB model can be applied to simulate the HAZ grain growth in welds. On the other hand, when the isothermal grain-growth kinetics are not available, the GBM

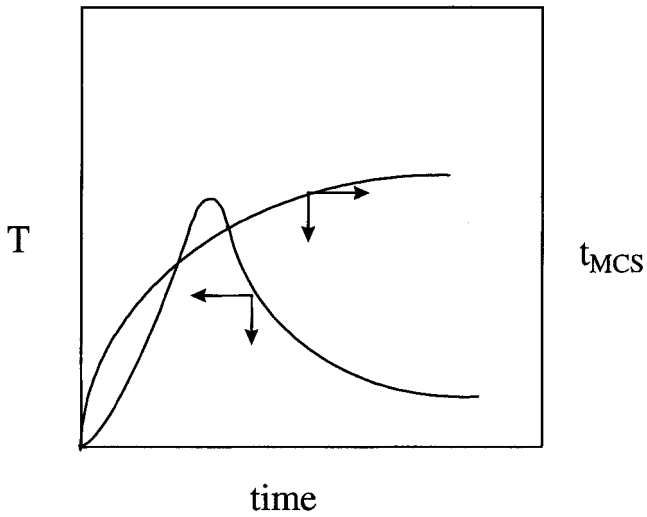

Fig. 1—A schematic diagram showing variation of temperature, T, and MC simulation time, t_{MCS}, with real time.

model is a good approach for grain-growth simulation. However, the physical properties of the material must be available. Furthermore, the model assumes the grain size to be proportional to the square root of time. One drawback of this model is that the assumed grain-growth exponent of 0.5 is not valid for many engineering alloys. For example, for most steels, the grain-growth exponent[8,9] has been found to be around 0.3. Therefore, the EDB model was adopted as the kinetic model to establish the relation between t_{MCS} and real time–temperature in the present investigation for a 2.25Cr-1 Mo steel.

1. *Description of EDB model*

According to the EDB model, a relation can be obtained, based on isothermal experimental data, between grain size (L), initial grain size (L_0), holding time (t), and temperature (T) by multiple regression analysis:

$$L^n - L_0^n = Kte^{\left(-\frac{Q}{RT}\right)} \qquad [8]$$

where K is a constant and Q is the activation energy. Both K and Q are obtained from experimental data. Substituting Eq. [4] into [8] and integrating it over an entire thermal cycle by summing the grain growth in short time intervals at different temperatures, a relationship between the MC simulation time and real time and temperature is obtained:

$$(t_{MCS})^{nn1} = \left(\frac{L_0}{K_1\lambda}\right)^n + \frac{K}{(K_1\lambda)^n}\sum\left(\Delta t_i e^{\left(-\frac{Q}{RT}\right)}\right) \qquad [9]$$

where T is the mean temperature in a time interval (Δt_i). Thus, at any given monitoring location where the temperature is known as a function of time, t_{MCS} can be related to real time ($t = \Sigma\Delta t_i$). Figure 1 is a schematic plot showing the variation of t_{MCS} with real time, calculated from Eq. [9] using the thermal cycle also shown in this figure.

2. *The MC simulation step and site-selection probability*

The t_{MCS} values at different locations, calculated from Eq. [9], cannot be directly applied in the MC algorithm. This is because the choice of a grid point for updating an orientation number is random in the MC technique, and, thus, the probability of selecting each grid point is the same in traditional MC calculations. However, grains must grow at higher rates in regions of higher temperature in the weld HAZ, where a steep temperature gradient exists. This fact must be included in any realistic grain-growth calculation scheme. One way to achieve this is to devise a scheme where grain orientations at higher-temperature locations (higher t_{MCS} locations) are updated more frequently by considering a probability gradient.[10] In other words, the site-selection probabilities vary with location. The larger the t_{MCS} at a site, the higher the corresponding site-selection probability ($p(r)$):

$$p(r) = \frac{t_{MCS}(r)}{t_{MCSMAX}} \qquad [10]$$

where $t_{MCS}(r)$ is the computed MC simulation time at the site with a distance of r from the heat source, and t_{MCSMAX} is the maximum MC simulation time.

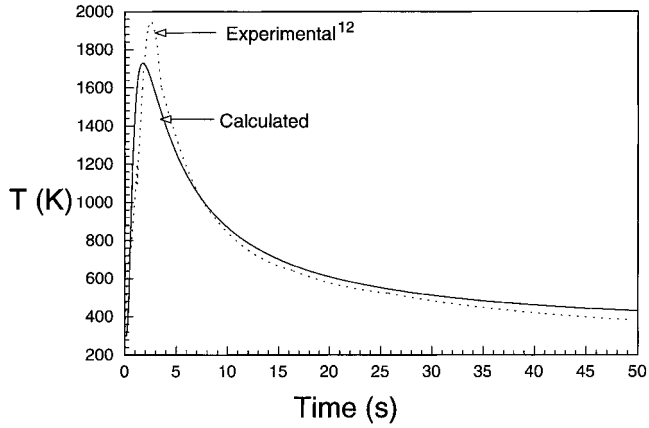

Fig. 2—Thermal cycle measured experimentally[12] and calculated for q/v = 1.1 MJ/m and r = 4.8 mm.

3. *Calculation of thermal cycles*

To determine the thermal cycles in the HAZ, the following equation, which represents the quasi–steady state 3-D heat conduction in a semi-infinite (very thick and large) work piece due to a moving point heat source,[17] was used.

$$T = T_0 + \frac{q}{2\pi k_s r} e^{-\frac{v(r-x)}{2\alpha_s}} \qquad [11]$$

This equation gives the temperature (T) as a function of welding speed (v) at any point at a distance of r from the heat source, which is assumed to be a point heat source. The symbol T_0 is the initial temperature (*i.e.* at $t = 0$), q is the heat input, k_s is the thermal conductivity, α_s (equal to $k_s/\rho c$) is the thermal diffusivity, ρc is the specific heat per unit volume, and r is given as

$$r = \sqrt{x^2 + y^2 + z^2} \qquad [12]$$

Figure 2 shows the computed and the experimentally determined thermal cycles for a heat input of $q/v = 1.1 \times 10^6$ J/m and at a distance of r = 4.8 mm from the heat source. The agreement shows that the calculation of temperature profiles using the heat-conduction equation is adequate. The material properties used for calculations are presented in Table I.

4. *Numerical Scheme*

In the present investigation, 3-D simulations were carried out in a simple cubic lattice system. The grid spacing (λ)

Table I. Data Used for the Physical Properties of a 2.25Cr-1Mo Steel[12]

Physical Property	Value
Thermal conductivity (k_s)	26 J m^{-1}
Specific heat per unit volume (ρc)	7.87×10^6 J m^{-3}
Melting point	1813 K
Activation energy (Q)	1.8×10^5 J mol^{-1}
Initial temperature	298 K
Experimental grain growth exponent (n)	3.17
Pre-exponential factor	2.19×10^{-3}

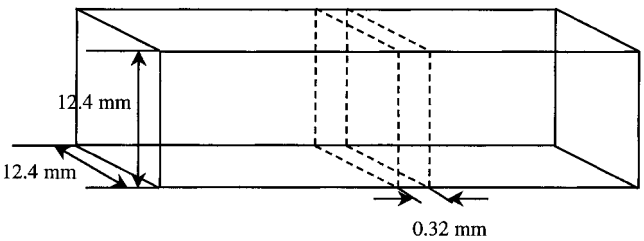

Fig. 3—Schematic of the calculation domain selected for the simulation of final grain structure. The dimensions of the selected domain are 0.32, 12.4, and 12.4 mm, respectively, and they correspond to a grid system of 40 × 1550 × 1550 grids.

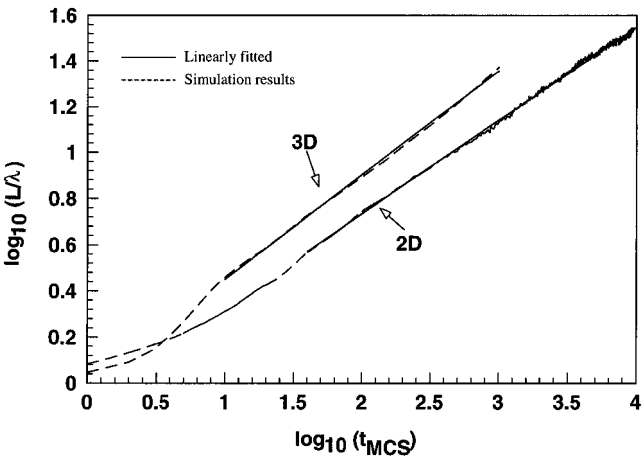

Fig. 4—A log-log plot of L/λ *vs* t_{MCS} for both 2-D (768 × 234) and 3-D (768 × 234 × 234) cases. The values of K_1 and n_1 are 0.82 and 0.40 for 2-D and 0.93 and 0.46 for 3-D, respectively.

was taken to be 8 μm, which is equal to the initial austenite mean grain size measured by Miranda and Fortes.[12] The calculation domain was chosen (shown as the thin dashed block in Figure 3) to be a slice from the region of the work piece, so that the calculation could be done with an 8 μm grid spacing. The grid system used to represent the calculation domain was 40 × 1550 × 1550 (which corresponds to (40 × 8 μm) × (1550 × 8 μm) × (1550 × 8 μm) = 0.32 × 12.4 × 12.4 mm^3, as shown in Figure 3).

a. *Determination of simulation constants*

Before simulation of grain growth under nonisothermal conditions, the dimensionless grain-growth kinetics from the present MC model under isothermal conditions needs to be established. In other words, the values of K_1 and n_1 in Eq. [4] need to be determined.

Figure 4 shows the simulated isothermal dimensionless grain-growth kinetics for the 40 × 1550 × 1550 grid system at 1443 K, which is the median temperature of the melting temperature (1813 K) and the austenite transformation temperature (1073 K). By plotting log (L/λ) as a function of log (t_{MCS}) in Figure 4, the values of the constants K_1 and n_1 in Eq. [4] are determined to be 0.93 and 0.46, respectively. Previous researchers have shown that the value of the grain-growth exponent n_1 lies in the range from 0.4 to 0.5 (0.47 for Yang *et al.*,[8] 0.46 for Radhakrishnan and Zacharia,[20] 0.41 for Grest *et al.*[19] in three dimensions, 0.48 for Gao *et al.*[8,9] (at very high t_{MCS}), and 0.41 for Anderson *et al.*[4] in two dimensions), depending on whether the grid system is 2-D or 3-D and on the number of MC simulation steps. As the number of neighbors increases, there is more interaction between the neighboring grains and, thus, grain growth is facilitated. Thus, for a 2-D calculation where the number of interactions with neighbors is less than that in a 3-D calculation, the value of the grain-growth exponent n_1 in 2-D calculations is less than in 3-D calculations for a fixed number of t_{MCS}. In previous studies,[19,20] it has been noted that, at low t_{MCS}, the initial grain size cannot be neglected in comparison to the mean grain size, which leads to a reduction in slope of the log-log plot between the mean grain size and t_{MCS}.

Finally, the grid size also influences the value of n_1. For very large grid systems (with more than a million grid points), the value of n_1 becomes independent of grid size.[18] This means that, for a very large grid system, the grain-size calculations become largely independent of grid size. Thus, similar grain-size gradients are observed even for different grid spacings (refer to Appendix II for a more detailed discussion).

The values of K_1 obtained by Radhakrishnan and Zacharia[20] were 0.84 for an isothermal 2-D system and 0.8 for an isothermal 3-D system, which are comparable to the values obtained in this study for K_1 (0.82 and 0.93, respectively). In addition to n_1 and K_1, there are other material-dependent constants which are obtained from isothermal experimental data. They are n, the experimental grain-growth exponent; K, the pre-exponential factor; and Q, the activation energy for grain growth. The values used for these constants for a 2.25Cr-1Mo steel are given in Table I.

b. *Distribution of* t_{MCS} and the probability

After knowing the value of the constants K_1 and n_1, the t_{MCS} values at each site were calculated from Eq. [9] by incorporating the corresponding thermal history into the equation. The distribution of the t_{MCS} in the cross section of the domain is shown in Figure 5(a). From this figure, it is observed that the maximum value of t_{MCS} lies at locations close to the fusion line. Near the fusion zone, t_{MCS} changes significantly due to a steep temperature gradient. After knowing the spatial distribution of t_{MCS} in the domain, the corresponding distribution of site-selection probability was obtained, using Eq. [10] as shown in Figure 5(b). As expected, the spatial distribution of the site-selection probability was similar to t_{MCS}. After obtaining the $p(r)$ distribution, the temperature-time history at each site was incorporated into the model by considering the spatial variation of the site-selection probability in the simulation domain.

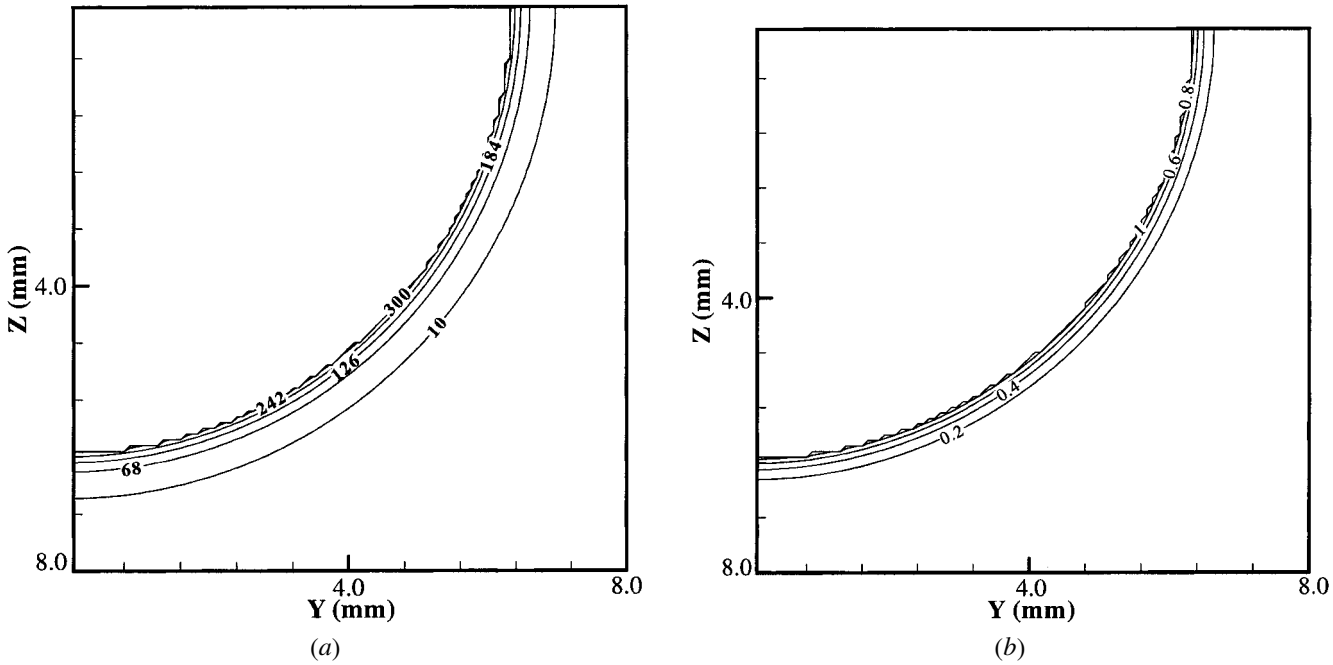

Fig. 5—Computed values of (*a*) spatial distribution of MC simulation time t_{MCS} and (*b*) site selection probability in the cross section perpendicular to the direction of welding. The calculations were done with a grid spacing of 8 mm and a grid system of 40 × 1550 × 1550 for a heat input of 4.2 MJ/m.

III. RESULTS AND DISCUSSION

The simulated final grain structure of the HAZ after the completion of welding is shown in Figure 6. Some regions of the HAZ have been magnified in the figure for clarity. The closer the site to the fusion line, the coarser the grain size. This is expected, since the grain-size change depends on the temperature. The higher the temperature at a site, the larger the final grain size. A continuous decrease of grain size with distance is observed.

Along the lines AB and CD on the top surface and vertical central plane directly under the fusion zone (shown in Figure 6), the calculated grain-size gradient is compared to experimental results in Figures 7 and 8 for different heat inputs. It is seen that the calculated results agree fairly well with the corresponding experimental data. The agreement indicates a significant promise for quantitative understanding of grain growth using 3-D MC simulation.

The extent of grain growth at various locations close to and equidistant from the fusion plane was significantly different, as shown in Figure 9. The grain growth on the top surface was not as pronounced as that on the central vertical plane directly under the fusion zone. For example, at a heat input of 1.9 MJ/m and a distance of 5.8 mm from the heat source, the mean grain size along the top surface (line AB) is 46 μm, but, along the central vertical plane (line CD) it is 56 μm. This behavior results from comparatively lower temperatures at the top surface than those below the heat source in the interior of the specimen. This result clearly shows the importance of doing calculations in three dimensions and the inherent problem of using a 2-D model to study grain growth in what is, in reality, a 3-D HAZ.

To further emphasize the importance of a 3-D calculation, simulations were done in both 2-D and 3-D (40 × 1550 and 40 × 1550 × 1550) domains to compute the grain-size variation with distance from the heat source. The results for simulation of grain growth in a 2D calculation are compared to the top surface of the 3-D domain for a q/v value of 1.9 MJ/m in Figure 10. This figure shows that the slope of the curve for a 3-D calculation is steeper than that for a 2D calculation. This difference results from the fact that the temperature gradients in a 2-D calculation are only in two dimensions, whereas, in a 3-D calculation, they are in three dimensions. So, the resulting grain-size gradient is more pronounced in three dimensions than in two dimensions. The figure also shows that, near the fusion line, the grain sizes are higher in a 3-D calculation. This is because of more neighboring interaction in a 3-D calculation than in a 2-D calculation. Also, the experimental results are in better agreement with the grain sizes calculated by the 3-D model than those calculated by the 2-D model.

Thermal pinning is the restriction of grain growth near the fusion plane due to steep temperature gradients.[13,14,15] As discussed earlier, near the fusion plane, the temperature gradients are very steep and the atomic mobility might vary even across a single grain. The thermal pinning effect tends to restrict the grain growth and, thus, tends to limit the grains from growing within a region with a sharp temperature gradient.

To examine this effect, simulations were done in a 3-D (40 × 1550 × 1550) domain, subjecting the whole domain to a thermal cycle at a distance of 6 mm from heat source (along line AB, as shown in Figure 6). The final mean grain size in the 3-D domain was around 54 μm (Figure 11). This value is comparatively greater than the mean grain size at the same distance (6 mm from the heat source along line AB, as shown in Figure 6) for a weld HAZ which was 36 μm (Figure 10). This difference can be attributed to the so-called thermal pinning effect, which takes place in the weld

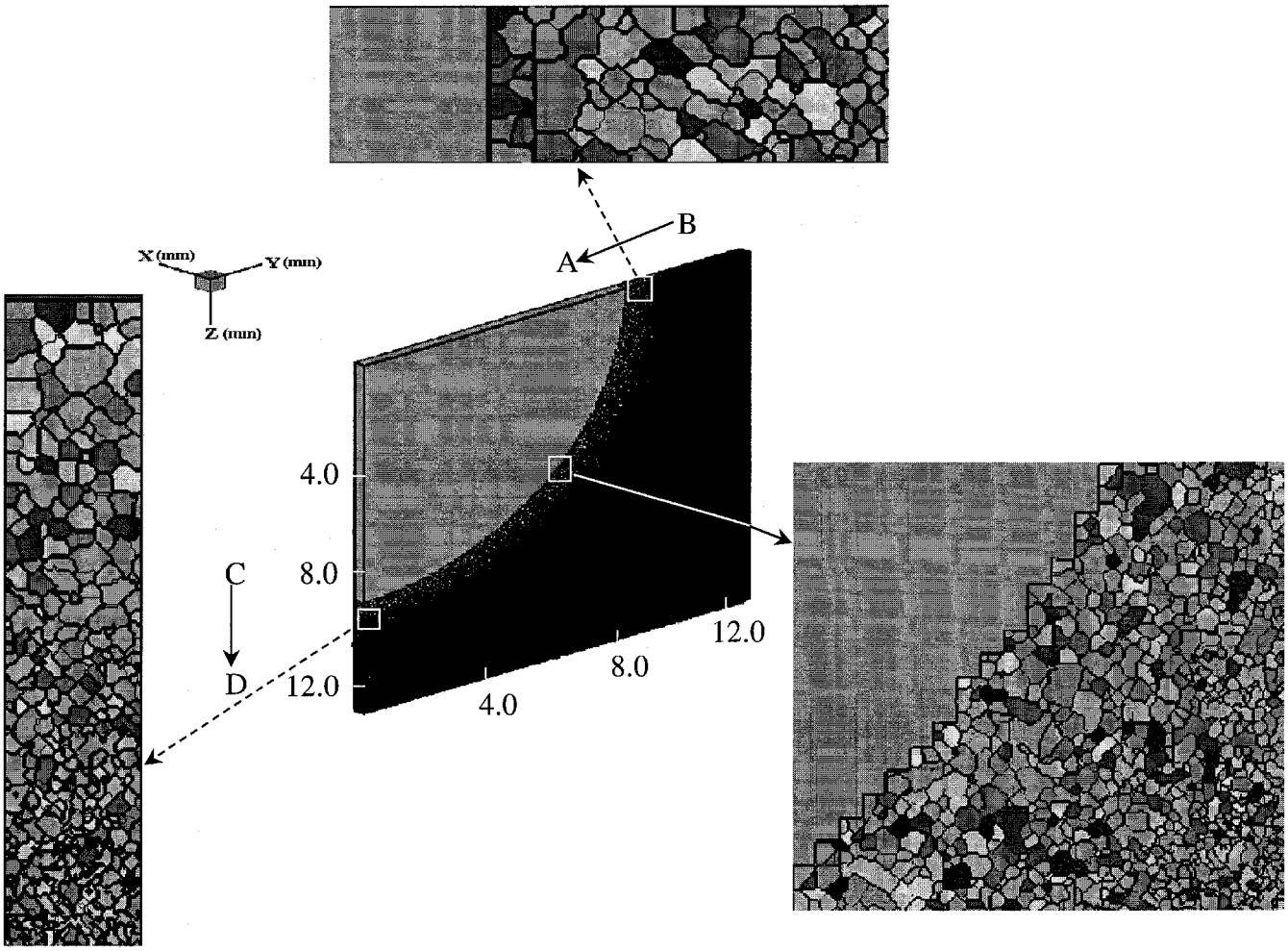

Fig. 6—Simulated HAZ grain structure after completion of welding. Some regions have been magnified for clarity. The heat input provided was 4.2 MJ/m and the grid spacing was 8 μm.

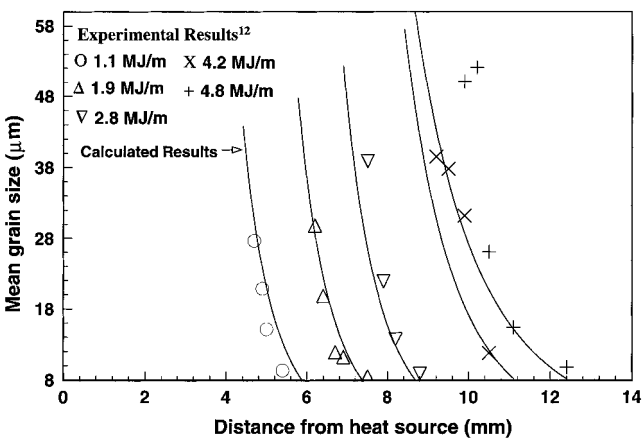

Fig. 7—Comparison of the calculated and experimental[12] mean grain size at various locations from the heat source. The calculated grain sizes were from the top surface of the sample (along line AB, as shown in Fig. 6).

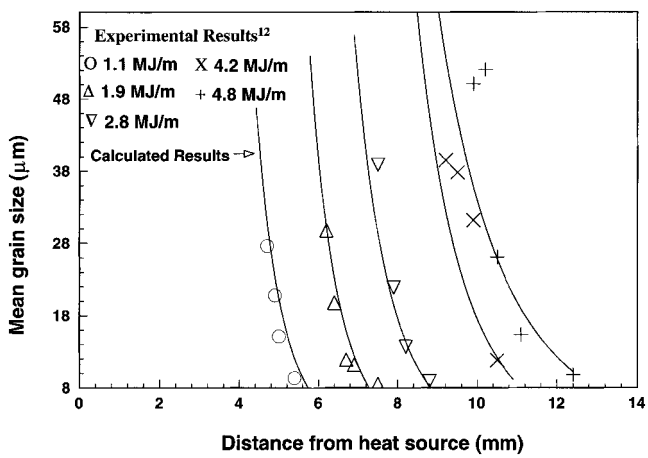

Fig. 8—Comparison of the calculated and experimental[12] mean grain size at various locations from the heat source. The calculated grain sizes were from the central vertical plane of the sample (along line CD, as shown in Fig. 6).

HAZ. The same effect was also observed in a 2D (40 × 1550) domain. The final mean grain size in the 2-D domain was around 49 μm (Figure 11) when the whole domain was subjected to the same thermal cycle, and that in the weld HAZ for the same 2-D domain was 34 μm (Figure 10). The difference between grain sizes obtained due to the thermal pinning in the 2-D and 3-D domains (Figure 11) can be attributed to the difference in the isothermal grain-growth exponents (0.40 in the 2-D case and 0.46 in the 3-D case).

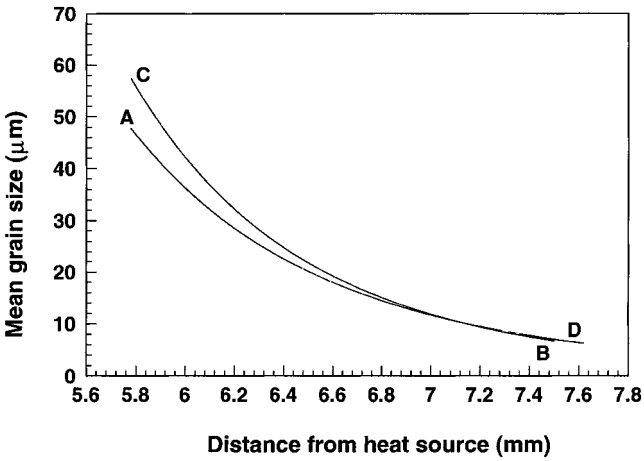

Fig. 9—Comparison between the mean grain size at different locations along the AB and CD lines (as shown in Fig. 6) at q/v = 1.9 MJ/m.

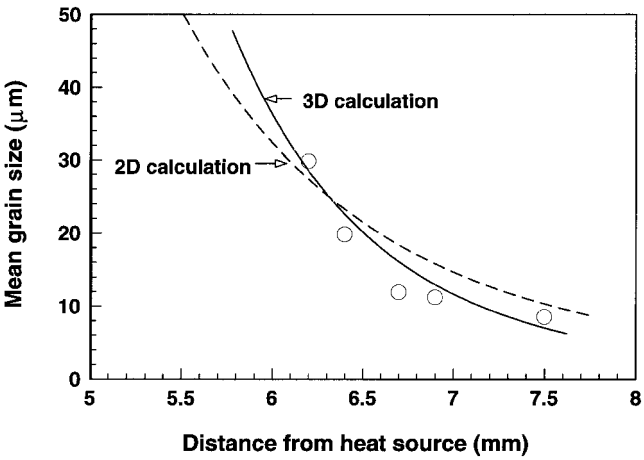

Fig. 10—The variation of grain size with the distance along line AB (as shown in Fig. 6) from the heat source for 2-D and 3-D calculations at a heat input of q/v = 1.9 MJ/m.

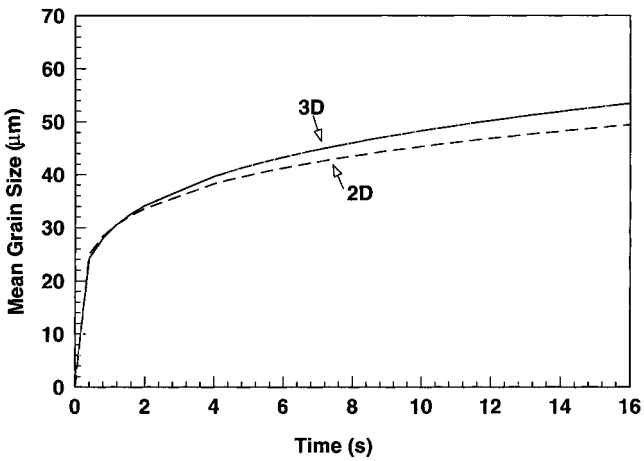

Fig. 11—The variation of computed mean grain size with time in 2-D and 3-D for a thermal cycle at a distance of 6 mm from the heat source (along line AB, as shown in Fig. 6) and q/v = 1.9 MJ/m. The plot exemplifies the effect of "thermal pinning," which takes place in the weld HAZ.

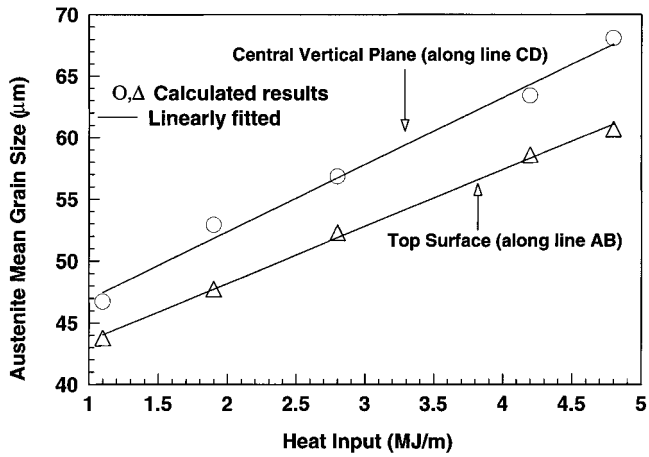

Fig. 12—Plot of the mean calculated austenite grain size produced in the HAZ of welds at 0.4 mm from the fusion plane as a function of heat input on two perpendicular planes.

The austenite grain size in the HAZ is controlled mainly by the heat input of the weld. The effect of heat input on the mean austenite grain size at 0.4 mm from the fusion plane is shown in Figure 12 for both the top surface (along the line AB, as shown in Figure 6) and the central vertical plane (along the line CD, as shown in Figure 6). There is a linear relationship between the mean grain size achieved and the heat input. When a very high heat input is used, such as at very low welding speeds, the HAZ becomes wide and grains coarsen significantly. This occurs because of two reasons. First, at very low welding speeds, the grains have more time to grow than at very high speeds, and, second, the high heat input produces higher temperatures, which helps the grain structure to coarsen. Also, it can be seen that there is more grain growth on the central vertical plane than on the top surface, due to comparatively lower temperatures on the top surface at all heat inputs.

IV. CONCLUSIONS

This article reports on the first 3-D modeling of grain growth in the HAZ of a steel weldment. The model simulates the evolution of grain structure in the entire HAZ under steep temperature gradients that cannot be obtained otherwise. Specifically, the grain growth in the HAZ of a 2.25Cr-1Mo steel weldment was investigated. The following are the main conclusions.

1. Both the computed results and independent experimental data[12] showed that the mean grain size near the fusion plane, for the welds considered in this investigation, was about 4 to 7 times larger than that in the base plate, depending on the experimental conditions, and it decreased continuously with distance from this plane. The computed grain size agreed well with the experimental data.[12]
2. Since the mean grain size at locations equidistant from the fusion line was different, all the previous 2-D calculations need to be re-examined. The computed mean grain-size values obtained from the 3-D calculations matched the experimental results more closely than the 2-D values.
3. Comparison of simulated isothermal grain-growth kinetics in the 2-D and 3-D models showed a lower value of

the grain-growth exponent n_1 in 2-D than in 3-D calculations, and this was attributed to the lesser number of neighbors for a 2-D grid point than for a 3-D one.

4. When an entire calculation domain was subjected to a thermal cycle calculated at a specific monitoring location, higher values of mean grain size were obtained than that obtained inside a weld HAZ that experiences the same thermal cycle. The restriction of grain growth under a temperature gradient, *i.e.*, thermal pinning, can be satisfactorily simulated by the present 3-D MC simulation.
5. The good agreement between the simulated grain structure and the corresponding experimental results indicates significant promise for understanding grain-growth phenomena in the entire HAZ, based on the 3-D MC technique.

ACKNOWLEDGMENTS

This research was supported by a grant from the United States Department of Energy, Office of Basic Energy Sciences, Division of Materials Sciences, under Grant No. DE-FGO2-84ER45158.

APPENDIX I

The value of the energy scale (J) related to the interfacial energy (γ) can be described as

$$J = \frac{\gamma}{ZN} \qquad \text{[Ia]}$$

where Z is the nearest-neighbor coordination number of the site and N is the number of atoms per unit grain-boundary area. For low-alloy steels (fcc), N is about[6] $2 \times 10^{19}/m^2$; Z, for the $\langle 111 \rangle$ plane of the 3-D fcc lattice, is 3; γ is 0.8 J/m^2; and the Boltzmann constant (k_B) is 1.381×10^{-23} J/K. Consequently, the value of J/k_BT in the temperature range from 973 to 1473 K is about 0.7 to 1. In this article, it was taken to be equal to unity.

APPENDIX II

It should be pointed out here that the value of the grid spacing adopted in the MC simulation will not significantly affect the final grain structure, as long as the final mean grain sizes are much larger than the grid spacing. This is because the effect of the value of the grid spacing has already been considered in determining the MC simulation step, as given in Eq. [9]. According to Eq.[9], the larger the value of λ, the smaller the t_{MCS} for simulation of grain growth under a specified welding condition. As a result, the predicted final grain structures should almost be the same, although different grid spacings are used. It should be recognized that a grid spacing larger than the average initial grain diameter after recrystallization is not particularly suitable for simulation of regions where the grain growth is rather limited. For example, the grain-growth process cannot be properly simulated in the regions where the final grain size is equal to or less than the selected grid spacing (far away from the fusion line).

REFERENCES

1. M.F. Ashby and K.E. Easterling: *Acta Metall.*, 1982, vol. 30, pp. 1969-78.
2. J.C. Ion and K.E. Easterling: *3rd Scand. Symp. in Materials Science*, 1983, pp. 79-85.
3. P.J. Alberry, B. Chew, and W.K.C. Jones: *Met. Technol.*, 1977, vol. 6, pp. 317-25.
4. M.P. Anderson, D.J. Srolovitz, G.S. Grest, and P.S. Sahni: *Acta Metall.*, 1984, vol. 32, pp. 783-91.
5. D.J. Srolovitz, M.P. Anderson, P.S. Sahni, and G.S. Grest: *Acta Metall.*, 1984, vol. 32, pp. 793-802.
6. Y. Saito and M. Enomoto: *Iron Steel Inst. Jpn. Int.*, 1992, vol. 32, pp. 267-74.
7. G.S. Grest, D.J. Srolovitz, and M.P. Anderson: *Acta Metall.*, 1985, vol. 33(3), pp. 509-20.
8. J. Gao and R.G. Thompson: *Acta Metall.*, 1996, vol. 44, pp. 4565-70.
9. J. Gao, R.G. Thompson, and Y. Cao: *Trends Welding Res.*, 1995, pp. 199-204.
10. B. Radhakrishnan and T. Zacharia: *Metall. Mater. Trans. A*, 1995, vol. 26A, pp. 2123-30.
11. A.L. Wilson, R.P. Martukanitz, and P.R. Howell: *Trends Welding Res.*, J.M. Vitek, S.A. David, J.A. Johnson, H.B. Smartt, and T. DebRoy, eds., ASM International, Materials Park, OH, 1998, pp. 161-66.
12. R.M. Miranda and M.A. Fortes: *Mater. Sci. Eng. A*, 1989, vol. 108, pp. 1-8.
13. P.J. Alberry and W.K.C. Jones: *Met. Technol.*, 1977, vol. 12, pp. 557-66.
14. P.J. Alberry and W.K.C. Jones: *Met. Technol.*, 1977, vol. 1, pp. 45-51.
15. K. Easterling: *Introduction to the Physical Metallurgy of Welding*, Butterworth and Co. Ltd., London, 1983, pp. 233-39.
16. X. Song and G. Liu: *Scripta Mater.*, 1998, vol. 38, pp. 1691-96.
17. T. DebRoy and S. Kou: *Welding Handbook*, ch. 3, in press.
18. Z. Yang, J.W. Elmer, J. Wong, and T. DebRoy: *Welding J. Res. Suppl.*, 2000, vol. 79(4), pp. 97s-117s.
19. G.S. Grest, M.P. Anderson, and D.J. Srolovitz: *Phys. Rev. B*, 1988, vol. 38, pp. 4752-60.
20. B. Radhakrishnan and T. Zacharia: *Metall. Mater. Trans. A*, 1995, vol. 26A, pp. 167-80.
21. ASTM Standard E 112-84, ASTM, Philadelphia, PA, 1984.